An algebraic approach for the motion control of the two-mass system

BARTÍK, O.

Proceedings IECON 2020 The 46th Annual Conference of the IEEE Industrial Electronics Society

eISBN: 978-1-7281-5413-8

DOI: https://doi.org/10.1109/IECON43393.2020.9255203

Accepted manuscript

An algebraic approach for the motion control of the two-mass system

1st Ondrej Bartik
CEITEC BUT
Brno University of Technology
Brno, Czech Republic
Email: ondrej.bartik@ceitec.vutbr.cz

***Abstract*—In this paper, an algebraic based approach for motion control of a two-mass system is presented. Algebraic menas, that the structure of the presented controller is found as the solution of the polynomial equation. The design approach is separated into two parts - velocity and position control design. Where for the velocity control the Model Reference Control schema with biquadratic filter is used. For the position control, a simple proportional controller is used. Described control schema also utilized an Anti-Windup mechanism together with controller output limitation to ensure torque (current) limit control. Firstly, the used model and method are described, then their application in the sense of the control design is described. Lastly, experimental results are presented and discussed.**

***Index Terms*—Two-mass, Model Reference Control, algebraic control, motion control**

I. Introduction

The two-mass system control design is the widely discussed topic in the last few decades. This type of system can be used as the model of the general mechanical load connected by a flexible link to the industrial electric drive systems. Work [1] can be used as the background for this problematic. Two-mass systems show (anti)resonance peaks on certain frequencies on their frequency characteristics because of their flexible character. This mainly limits the range of the closed-loop controlled system bandwidth with the classic PID control structures as it is shown in: [2]. There are several basic methods to workaround this issue with (anti)resonance behavior. For the survey of these basic methods see: [3]. In nutshell, these methods either use a low-pass filter or a notch filter to suppress the resonance peaks in frequency characteristics, or use a different type of filter (biquadratic filter) to exactly match and cancel out some members or part of the controlled plant transfer functions which cause the flexible behavior. Or another group of methods is based on usage of additional acceleration feedbacks to cancel out the undesirable oscillation from the drive torque, shaft velocity and optionally, from the shaft angular position as well. As the source of the acceleration feedback, an extra sensor or appropriate observer can be used. The observers are usually used to decrease the price of the drive system. An example of the low-pass filter usage can be found in: [4]. Or the combination of two biquadratic filters with classic PI controller is described here: [5]. A notch filter is also often used filter to improve closed loop performance. As the example, see this work: [6]. Few works focused on using additional acceleration feedback with an appropriate torque observer: [7], [8], and [9]. The main drawback of low-pass filters is the negative contribution to the phase margin. See [3] for details. The common problem of observer-based methods is the necessity of derivative estimate implementation, which leads to noise amplification and limits the usage of this approach. Again, for more details see [3]. Another group of methods is based on algebraic design approaches. Following work: [10] can be used as an example of the polynomial based method. The main drawback of algebraic based design methods is the Windup effect. This is because of the structure of the controller which can be given by polynomials. So it can be impossible to implement classic clamping and back-calculation methods. Hence, some special approaches must be used. The resulted control structure complexity (given by algebraic design approach) can be understood as another drawback due to the implementation issues. Or following work [11] use the H_∞ approach.

This paper presents a solution that uses the algebraic design approach in combination with the appropriate biquadratic filter altogether with appropriate Anti-Windup mechanism to establish velocity control for a two-mass system that is able to work within the torque (current) limitation. The biquadratic filter is used to simplify resulted control structure given by the algebraic design. This method uses a given reference model as the pattern of the closed-loop behavior. The method itself uses a generic control structure to match the closed-loop behavior with the reference model transfer function. For the purposes of this paper, a second-order low-pass filter is used as the reference model. For the purposes of the position control design, a simple proportional (P) controller is used. The design of this controller is focused on the closed-loop response aperiodicity. Detailed information about the control design methodology can be found in Section III. As it is, the methodology described in this paper can easily fit an idea of so-called smart system integration for mechatronic

This work was supported by the ECSEL Joint Undertaking under Grant 737453/8A17003 (I-MECH). This research also has been financially supported by the Ministry of Education, Youth and Sports of the Czech republic under the project CEITEC 2020 (LQ1601). and also the completion of this paper was made possible by the grant No. FEKT-S-20-6205 - "Research in Automation, Cybernetics and Artificial Intelligence within Industry 4.0" financially supported by the Internal science fund of Brno University of Technology.

applications, see: [12].

The presented methodology is demonstrated through the real experiment on the testbench formed by the Permanent Magnet Synchronous Motor (PMSM) used as the source of the torque and with the flywheel as the load connected via a long thin shaft to the PMSM as the flexible connection between the load and the PMSM. Section IV contains experimental results of the designed velocity and position control.

The electrical part of the PMSM is omitted and abbreviated in this paper since this paper is oriented on the drive system mechanical part only. The considered abbreviation of the electrical part is described in Section III-C. Another field that is omitted in this paper is plant parameter identification as this paper is focused mainly on the control design methodology. The plant parameters are given in Table I.

II. Model and Method Description

A. Two-mass system model

For the two-mass model, well known and simplified form [1] (backlash excluded) is used. Nevertheless, the model includes the elasticity coefficient as well as the coefficient of dumping. Model is described by the following set of three equations:

$$J_m \frac{d\omega_m}{dt} = T_i - b(\omega_m + \omega_l) - k(\vartheta_m - \vartheta_l) \tag{1}$$

$$J_l \frac{d\omega_l}{dt} = b(\omega_m + \omega_l) + k(\vartheta_m - \vartheta_l) \tag{2}$$

$$\omega_{m,l} = \frac{d\vartheta_{m,l}}{dt} \tag{3}$$

where J_m $[\mathrm{kg}\cdot\mathrm{m}^2]$ and J_l $[\mathrm{kg}\cdot\mathrm{m}^2]$ are inertias of the first and second mass respectively, ω_m $[\mathrm{rad}\cdot\mathrm{s}^{-1}]$ and ω_l $[\mathrm{rad}\cdot\mathrm{s}^{-1}]$ are angular velocities of the first and second mass respectively, and ϑ_m [rad] and ϑ_l [rad] are angular positions of the first and second mass respectively. Parameter k $[\mathrm{kg}\cdot\mathrm{m}^2\cdot\mathrm{s}^{-2}]$ is coefficient of elasticity and parameter b $[\mathrm{kg}\cdot\mathrm{m}^2\cdot\mathrm{s}^{-1}]$ is coefficient of dumping. Equation (1) describes torque applied on the first mass and equation (2) describes torque applied to the second mass. The system can be understood as the system with a single input (torque generated by electromagnetic part of the motor) and with two outputs (velocity of each mass). Hence two different transfer functions can be derived.

$$G_{pm} = \frac{\omega_m}{T_i} = \frac{1}{J_m + J_l} \cdot \frac{J_l s^2 + bs + k}{J_c s^3 + bs^2 + ks} \tag{4}$$

$$G_{pl} = \frac{\omega_l}{T_i} = \frac{1}{J_m + J_l} \cdot \frac{bs + k}{J_c s^3 + bs^2 + ks} \tag{5}$$

where $J_c = \frac{J_m J_l}{J_m + J_l}$. Last set of equations express the resonant and anti-resonant angular frequencies:

$$\omega_{ar} = \sqrt{\frac{k}{J_l}} \tag{6}$$

$$\omega_r = \sqrt{\frac{k}{J_c}} \tag{7}$$

One can see, that $J_l > J_c$ for any J_m and J_l. This follows that $\omega_r > \omega_{ar}$, for any case of used load.

B. MRC schema

This method belongs to the group of the pole-placement methods and contemplates plant in the following form:

$$G_p(s) = k_p \frac{Z_p(s)}{R_p(s)} \tag{8}$$

where k_p is a constant, Z_p is the monic and Hurwitz numerator polynomial and R_p is the monic denominator polynomial. The method also presents a control structure given by the following control variable formula u_p:

$$u_p = \boldsymbol{\theta_1}^T \frac{\boldsymbol{\alpha}(s)}{\Lambda(s)} u_p + \boldsymbol{\theta_2}^T \frac{\boldsymbol{\alpha}(s)}{\Lambda(s)} y_p + \theta_3 y_p + c_0 r \tag{9}$$

where $\boldsymbol{\theta_1}, \boldsymbol{\theta_2} \in \mathbb{R}^{n_p-1}; \theta_3, c_0 \in \mathbb{R}^1$ are parameters which need to be designed. $\Lambda(s)$ is an arbitrary polynomial with the degree $n_p - 1$ and y_p and r are plant output and closed loop reference input respectively. Lastly, $\boldsymbol{\alpha}(s)$ is defined as follows:

$$\boldsymbol{\alpha}(s) = \begin{cases} [s^{n_p-2}, s^{n_p-3}, \cdots, s, 1]^T & n_p \geq 2 \\ \mathbf{0} & n_p = 1 \end{cases} \tag{10}$$

where s is Laplace operator. The main objective of this method is to design $\boldsymbol{\theta_1}$, $\boldsymbol{\theta_2}$, θ_3, and c_0 in such a way, that closed-loop transfer function $G_c(s)$ equates arbitrary reference model $G_m(s)$, i.e.:

$$\frac{c_0 k_p Z_p \Lambda}{(\Lambda - \boldsymbol{\theta_1}^T \boldsymbol{\alpha}) R_p - k_p Z_p (\boldsymbol{\theta_2}^T \boldsymbol{\alpha} + \theta_3 \Lambda)} = k_m \frac{Z_m(s)}{R_m(s)} \tag{11}$$

where the left side express the transfer function of the closed-loop and the right side expresses the reference model with k_m as the high-frequency gain, Z_m as the monic and Hurwitz numerator polynomial and R_m as the monic and Hurwitz denominator polynomial. According to [13], the parameter c_0 is usually chosen as the $c_0 = \frac{k_m}{k_p}$. The relative degree of the $G_p(s)$ and $G_m(s)$ has to be the same. With $\Lambda = Z_m \Lambda_0$, the equation (11) can be rewritten as follows:

$$(\Lambda - \boldsymbol{\theta_1}^T \boldsymbol{\alpha}) R_p - k_p Z_p (\boldsymbol{\theta_2}^T \boldsymbol{\alpha} + \theta_3 \Lambda) = Z_p \Lambda_0 R_m \tag{12}$$

The solution of the $\boldsymbol{\theta_1}, \boldsymbol{\theta_2}, \theta_3$ can be found by equating of the powers coefficients on the both sides of (12). The main drawback of this method is, that for high order plants, the $\boldsymbol{\alpha}$ vector contains high power of s which represents high order derivatives and this causes undesired noise amplification at the real implementation. This leads to the poor feasibility for

the high order plants. On the other hand, this method ensures pole-zero cancelation only in $\mathbb{C}^-$. The tracking error which is the error between the plant and the model outputs $e_{tr} = y_p - y_m$ converges exponentially fast to zero [13] and the rate of convergence is described by the following equation:

$$\Lambda(s)\Lambda_0(s)R_m(s)Z_p(s) = 0 \tag{13}$$

The (13) is the characteristic polynomial of e_{tr}. The proof for this is omitted in this paper for its length. But it can be found here [13]. As one can see from (13), the rate of convergence can be influenced by the user choice of the Λ_0 and R_m polynomials.

III. Experiment description

A. Control design

The main objective of this paper is to present movement (velocity and position) control of the two-masssystem. Therefore, the control of the electric part of the PMSM is omitted and the whole controlled electric part of the plant is abbreviated to the single scalar constant K_i $[\mathrm{Nm} \cdot \mathrm{A}^{-1}]$ which is torque current constant of the PMSM. Anyway, it is considered that the PMSM is controlled via field-oriented control, where d-axis current i_d is kept zero and q-axis current i_q is torque generating current, which is considered as the input for the plant $G_p^*(s)$. The relation between q-axis current and generated torque is given by the following formula:

$$T_i = i_q K_i \tag{14}$$

The purpose of the designed controller is to control the velocity and position of the second mass of the two-mass system. Firstly, the velocity control is designed. The plant for this task is given as follows:

$$G_p^* = \frac{\omega_l}{i_q} = \frac{K_i}{J_m + J_l} \cdot \frac{bs + k}{J_c s^3 + bs^2 + ks} \tag{15}$$

this transfer function represents a third-order system with a second-order relative degree. To use the control scheme described in the II-B the reference model has to be of second-order relative degree as well. The second-order system with no zeros appears as the most simple option. But order of the plant n_p leads to $\alpha(s) = \begin{bmatrix} s, & 1 \end{bmatrix}^T$, which introduces a derivative into the control structure. And as it was mentioned before, this causes undesired noise amplification and decreases the feasibility of the controller. The use of the proper bi-quadratic (biquad) filter appears as a possible workaround. Consider the biquad filter $G_f(s)$ given by the following transfer function:

$$G_f(s) = \frac{J_c s^2 + bs + k}{b\sqrt{\frac{J_c}{k}}s^2 + (\sqrt{kJ_c} + b)s + k} \tag{16}$$

Now, if this filter is applied on the input of the plant given by (15), with (7) the plant is changed into:

$$G_p(s) = \frac{K_i \omega_r}{J_m + J_l} \cdot \frac{1}{s^2 + \omega_r s} \tag{17}$$

Now, the order n_p is decreased by one and relative order is still equal to two. Again, the use of the second-order system with no zeros as the reference model appears as the most simple option. Moreover, according to (10), $\alpha = 1$ which does not cause any problem in the control structure linked with the derivatives. And also $\boldsymbol{\theta_1}, \boldsymbol{\theta_2} \in \mathbb{R}^1$. Now, the reference model $G_m(s)$ is chosen as the:

$$G_m(s) = \frac{(\Gamma_m \omega_r)^2}{(s + \Gamma_m \omega_r)^2} \tag{18}$$

where Γ_m is an arbitrary integer and $\Gamma_m > 0$. Now let k_p, k_m and polynomials R_p, Z_p, R_m, Z_m be set with (17) and (18) as follows:

$$\begin{aligned} k_p &= \frac{K_i \omega_r}{J_m + J_l} \\ R_p &= s^2 + \omega_r s \\ Z_p &= 1 \\ k_m &= (\Gamma_m \omega_r)^2 \\ R_m &= (s + \Gamma_m \omega_r)^2 \\ Z_m &= 1 \end{aligned} \tag{19}$$

Finally, let $\Lambda_0 = s + \Gamma_m \omega_r$ and as it was said before, $\alpha = 1$. Now with (11), the $\boldsymbol{\theta_1}$, $\boldsymbol{\theta_2}$, and θ_3 can be found as:

$$\begin{aligned} \boldsymbol{\theta_1} &= (1 - 2\Gamma_m)\omega_r \\ \boldsymbol{\theta_2} &= (2\Gamma_m^3 \omega_r^3 - 3\Gamma_m^2 \omega_r^3 + \Gamma_m \omega_r^3) k_p^{-1} \\ \theta_3 &= (3\Gamma_m \omega_r^2 - 3\Gamma_m^2 \omega_r^2 + \omega_r^2) k_p^{-1} \end{aligned} \tag{20}$$

The parameter Γ_m can be understood as the closed-loop bandwidth scale. The higher the value of Γ_m is, the higher the cutoff frequency of (18) is. For $\Gamma_m = 1$ the cutoff frequency is set to ω_r and the closed-loop bandwidth "embraces" the frequency span from low frequencies over the ω_{ar} up to the ω_r.

The position control is ensured by a simple proportional controller. The controller is designed with regard to the aperiodicity of the transient response of the closed-loop system. With the consideration that the velocity control closed-loop transfer function is equal to the reference model given by (18), then the position control closed-loop transfer function with the proportional controller is given by:

$$G_{c,pos} = \frac{P(\Gamma_m \omega_r)^2}{(s + \Gamma_m \omega_r)^2 s + P(\Gamma_m \omega_r)^2} \tag{21}$$

where P is the proportional gain of the controller. The transient behavior of the closed-loop system is in this case given only by the denominator polynomial. To ensure aperiodic behavior of transient response, there must by no complex

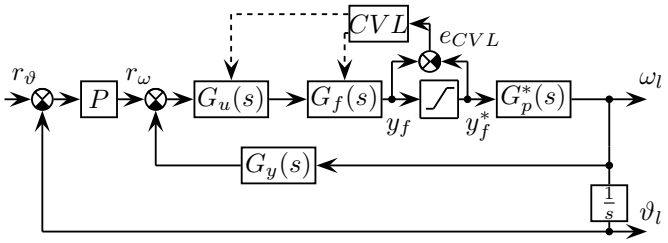

Fig. 1. Control structure with the anti-windup mechanism

pole-pairs in the denominator polynomial. Based on the well-known theory of cubic equation and the abilities of the cubic discriminant it follows that if the discriminant is equal to zero there are only real roots and some of them are multiple roots. If the P is set as $P = \frac{4}{27}\Gamma_m\omega_r$, then the discriminant of denominator of (21) is zero and (21) can be rewritten as follows:

$$G_{c,pos} = \frac{4}{27} \cdot \frac{(\Gamma_m\omega_r)^3}{(s + \frac{1}{3}\Gamma_m\omega_r)^2(s + \frac{4}{3}\Gamma_m\omega_r)} \tag{22}$$

which gives us closed-loop transfer function of position control. Again, closed-loop bandwidth and transient response performance is tied with the value of Γ_m.

B. Limited torque control

Block $G_f(s)$ can sometimes suggest an inappropriate output value applied at the plant input. Inappropriate means, that the value is higher than the maximum value of current which PMSM is able to work with. For this purpose, the output of $G_f(s)$ must be limited with the saturation at the maximum admissible value. To deal with the Control Value Limitation (CVL) effect tied with the saturated output of block $G_f(s)$ there is the appropriate mechanism. A similar technique to the one described here: [14] was used. On Fig. 1, the whole control structure is depicted, where blocks $G_u(s)$ and $G_y(s)$ are given by the following set of transfer functions:

$$\begin{aligned} G_u(s) &= \frac{k_m}{k_p} \cdot \frac{1}{1 - \boldsymbol{\theta_1}\frac{\boldsymbol{\alpha}}{\Lambda_0(s)}} = \frac{(\Gamma_m\omega_r)^2}{k_p} \cdot \frac{s + \Gamma_m\omega_r}{s - \omega_r + 3\Gamma_m\omega_r} \\ G_y(s) &= \theta_3 + \boldsymbol{\theta_2}\frac{\boldsymbol{\alpha}}{\Lambda_0(s)} = \frac{\frac{3\Gamma_m^2 - 3\Gamma_m + 1}{\Gamma_m^2}s + \Gamma_m\omega_r}{s + \Gamma_m\omega_r} \end{aligned} \tag{23}$$

Further, from Fig. 1, r_θ, r_ω stand for the reference position and velocity inputs respectively and ω_l, ϑ_l are velocity and position of the second mass of the two-mass system respectively. The block CVL stands for Control Value Limitation mechanism which influences blocks $G_u(s)$ and $G_f(s)$. Signal e_{CVL} is used to detect the current limitation exceeding.

For the purpose of the $G_f(s)$ output limitation, let y_f be the output of the biquad $G_f(s)$ and y_f^* be the output of the saturation block defined as follows:

$$y_f^* = \begin{cases} i_{max} & e_{CVL} > 0 \\ y_f & e_{CVL} = 0 \\ -i_{max} & e_{CVL} < 0 \end{cases} \tag{24}$$

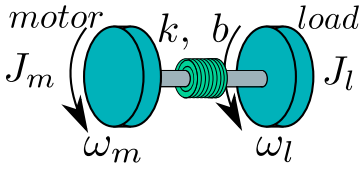

Fig. 2. Two-mass mechanical load illustration

TABLE I
TESTBENCH PARAMETERS

Parameter	Value	Parameter	value
T_n	$1.15\ \mathrm{N \cdot m}$	i_n	$8.5\ \mathrm{A}$
K_i	$1.35\ \mathrm{N \cdot m \cdot A^{-1}}$	Jm	$6.5 \cdot 10^{-5}\ kg \cdot m^2$
Jl	$1.3 \cdot 10^{-3}\ \mathrm{kg \cdot m^2}$	J_c	$6.2 \cdot 10^{-5}\ \mathrm{kg \cdot m^2}$
k	$6.8\ \mathrm{kg \cdot m^2 \cdot s^{-2}}$	b	$0.003\ \mathrm{kg \cdot m^2 \cdot s^{-1}}$

where i_{max} stands for the maximum admissible current value. Also, when $e_{CVL} \neq 0$, the input value of the $G_u(s)$ is back-calculated through the blocks $G_f(s)$ and $G_u(s)$ to match the value of $\pm i_{max}$ which is forced at the output of the $G_f(s)$ by (24). This artificial input value is used as the regular input value for the $G_u(s)$ block in the next step of control algorithm as long as the $e_{CVL} \neq 0$. This ensures limited current or rather limited torque control, where relation between current and torque generated by the PMSM is given by (14). For the purpose of the implementation, blocks $G_u(s)$, $G_f(s)$ and $G_y(s)$ are discretized with the forward euler method. The dashed lines in Fig. 1 symbolize the indirect impact of block CVL on the controller blocks. It means that block CVL does not change the parameters of the $G_u(s)$ and $G_f(s)$, but it only forces these blocks to use different input values.

C. Testbench description

For the testbench purposes, the TGT3-0130 PMSM was used. Long and thin shaft was connected to the PMSM shaft by the first end and the $1\ \mathrm{kg}$ flywheel with $10\ \mathrm{cm}$ diameter was connected to the second end. The long and thin shaft makes up a flexible connection between the mass formed by the PMSM shaft inertia and the mass formed by the flywheel inertia like it is shown in Fig. 2. Values of the nominal current i_n, the nominal torque T_n, and the torque-current constant K_i of the PMSM altogether with the values of k, b, J_m, and J_l can be found in Table I.

the HENNGSTLER RI58-O/5000A quadrature optical encoder was used as the motion sensor, connected to the second mass, the flywheel. The encoder has 5000 pulses per revolution, which gives 20000 edges to detect. For better angular position accuracy of the shaft and velocity estimation of the shaft, the angle tracking observer with the first-order Butterworth filter was used. For more details about angle tracking observer structure and tunning, please see [15]. To unite testbench with the control structure in Fig. 1, the filtered shaft angular position from angle tracking observer is considered as the ϑ_l signal and observed shaft velocity from angle tracking observer is considered as the ω_l signal. The dynamics of the observer is omitted and considered as it has no effect on the dynamic behavior of $G_p^*(s)$.

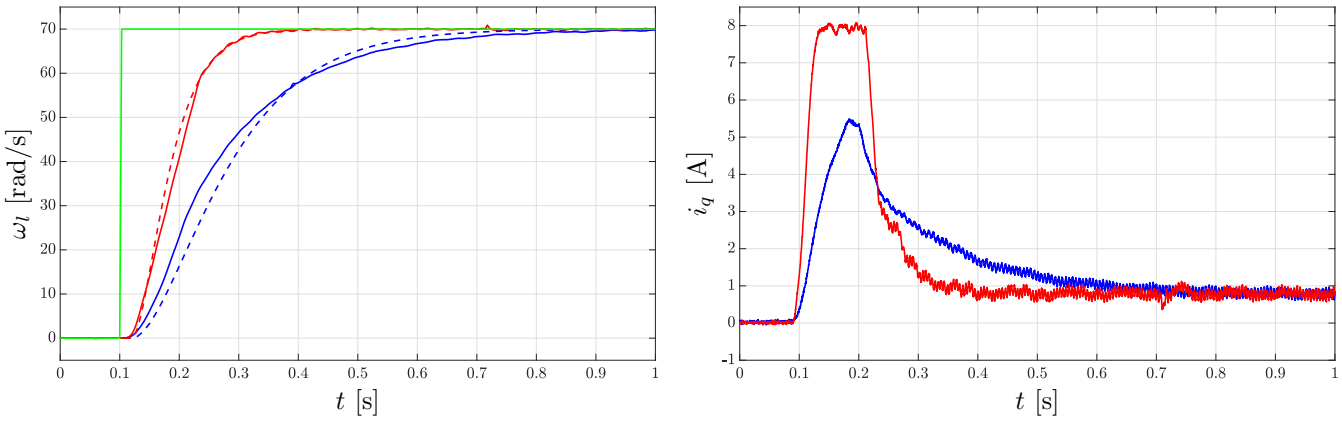

(a) (b)

Fig. 3. The velocity (a) and current (b) responses for the velocity step command. Blue lines stand for the responses with $\Gamma_m = 2$ and red lines stand for responses with $G_m = 7$. The dashed lines are responses of models $G_m(s)$ with corresponding Γ_m values. The green solid line stands for command value.

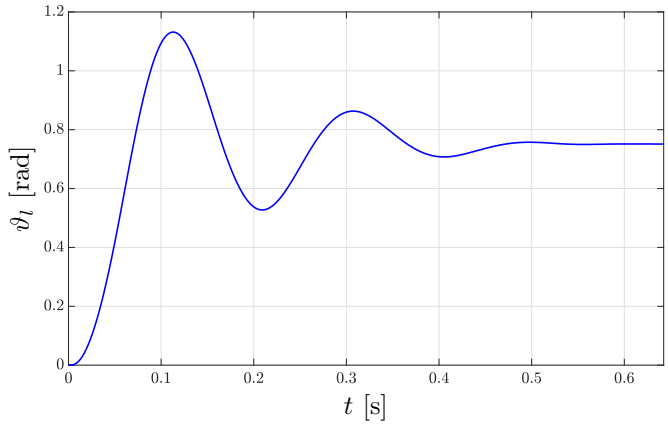

Fig. 4. Second mass angle position response due to the rotor alignment

IV. Results and Discussion

All results were acquired from the dSpace RTI1103 platform with acquisition frequency equal to 4 kHz. For a better image of the system flexibility, see Fig. 4. The second mass angle position response during the rotor alignment is depicted in this figure. As the design of the individual control schemes (velocity and position) were separated, the discussion about the results will be separated in the same way.

Firstly, in Fig. 3 there are velocity step command responses for different values of the Γ_m parameter altogether with i_q responses. Where the step command was 70 [rad/s]. The transient of the difference between the reference model output y_m and the measured plant output y_p (tracking error e_{tr}) is, as was mentioned in II-B, dependent on the choice of the R_m and Λ_0 polynomials. But of course, the transient behavior of e_{tr} is dependent on the omitted dynamics of the electrical part and on the static friction of the PMSM, which was omitted as well. The choices of $\Lambda_0(s)$, $R_m(s)$, $Z_p(s)$ and $Z_m(s)$ stated in the section III change equation (13) into:

$$(\Gamma_m \omega_r s + 1)^3 = 0 \tag{25}$$

Now, Γ_m can be also understood as the scale of tracking error e_{tr}, which means the higher the values of Γ_m is, the faster convergence of y_p to y_m is. But unsurprisingly, the higher the value of Γ_m is, the higher the value of the current i_q is demanded. Fig. 3 (b) shows that the saturation mechanism together with the described anti-windup algorithm ensures limited current value and stable velocity response. Of course, Anti-Windup and limitation in current can be understood as non-linear elements and as such, they also have an impact on the tracking error e_{tr} transient. Anyway, the rising time of the velocity step command response is approximately 200 ms with $\Gamma_m = 7$. Because the value of the current i_q is already saturated within its limit, the torque cannot be any higher and the acceleration, respectively the rising time of the velocity command response is limited as well.

Secondly, in Fig. 5 the step responses of the position control altogether with the corresponding i_q currents can be observed. Fig. 5 (a) depicts position step command responses for $\Gamma_m = 5$ (blue solid line) and $\Gamma_m = 15$ (red solid line). The position step command was set to $\frac{\pi}{3}$ [rad]. Dashed lines represent the models given by (21) with appropriate values of the Γ_m. Again, some mismatches between the obtained responses and models can be observed. This is caused by the same problems as in the case of velocity control. Moreover, as the velocity closed-loop transfer function does not match reference model (18) transfer function perfectly, the ensuring of the condition of aperiodicity and matching of the position closed-loop with the presumed shape of the transfer function (21) by choosing $P = \frac{4}{24}\Gamma_m \omega_r$ is not perfect as well. Nevertheless, for the $\Gamma_m = 15$ the step response of the position control still shows no significant overshoots and rising time for step command $\frac{\pi}{3}$ [rad] is approximately 150 ms. The impact of the Γ_m parameter on the position closed-loop dynamics is clearly given by (21).

The main advantage of this concept is that velocity closed-loop dynamics, position closed-loop dynamics, and the tracking error e_{tr} convergence is controlled only by the single parameter, Γ_m. In theory, the higher the value of Γ_m is, the faster the transient responses are and the matching of the plant

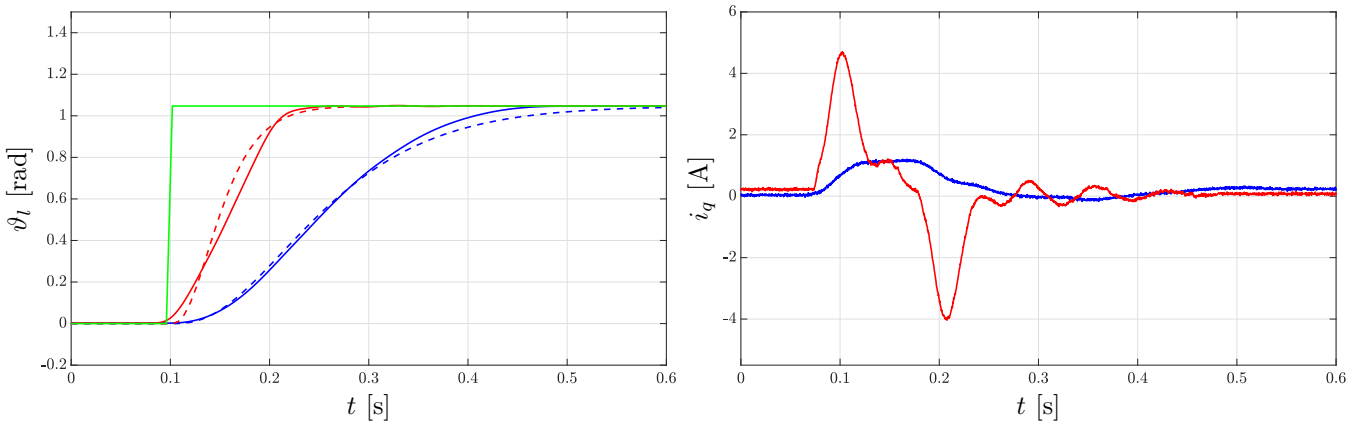

(a) (b)

Fig. 5. Position (a) and current (b) responses for the position step command ($\pi/3$). Blue lines stand for the responses with $\Gamma_m = 5$ and red lines stand for responses with $G_m = 18$. The dashed lines are responses of closed-loop models (21) with a corresponding Γ_m values. The green solid line stands for command value.

output with the reference model output is better. And of course, with better plant output and reference model output matching, the position closed-loop transfer function is closer to the one given by (21). Nevertheless, in this case, the value of torque generated by PMSM is limited and hence it is pointless to set the value of Γ_m uselessly high because the peak value of the torque (i_q current) applied to the plant is linked with the value of Γ_m parameter. And this leads to the same conclusion as the discussion about the velocity control design results. So, that the rising time of step command responses cannot be any higher because the amount of torque applied to the plant (acceleration) cannot be any higher. The only way to speed up the output responses is to speed up the current ramp up. But according to Fig. 3, the time gain would be 10 ms approximately.

V. Conclusion

This paper presents an algebraic approach of the motion control design for a two-mass system. The presented methodology was demonstrated on the real testbench. Design methodology is separated into two steps. Firstly, the velocity control design is described where the Model Reference Control schema combined with biquadratic filter was used. Secondly, the position control is described were the simple proportional controller was used. An Anti-Windup mechanism was added into the velocity control structure to ensure the stable and satisfying functionality under the torque (current) limitation. The velocity control was designed to match the dynamical behavior between the velocity closed-loop and the given reference transfer function. The position control was designed with the focus on the aperiodicity of the transient response of the closed-loop system. The whole design methodology is described in detail in Section III. All the results were presented graphically via appropriate figures and also were discussed in section IV.

References

[1] A. Boutros, P. El-Jurdi, H. Y. Kanaan, and K. Al-Haddad, "Modeling and simulation of a complex mechanical load using the multi-mass approach," *Proceedings of the Mediterranean Electrotechnical Conference - MELECON*, no. April, pp. 373–379, 2014.

[2] P. I. D. Control, G. Zhang, and J. Furusho, "Speed Control of Two-Inertia System," vol. 47, no. 3, pp. 603–609, 2000.

[3] G. Ellis and R. D. Lorenz, "Resonant load control methods for industrial servo drives," *Conference Record - IAS Annual Meeting (IEEE Industry Applications Society)*, vol. 3, pp. 1438–1445, 2000.

[4] W. Y. Wang and A. W. Shen, "Detection and reduction of middle-frequency resonance for industrial servo with self-tuning lowpass filter," *Journal of Control Science and Engineering*, vol. 2012, 2012.

[5] M. Giacomelli, D. Colombo, G. Finzi, V. Šetka, L. Simoni, and A. Visioli, "An autotuning procedure for motion control of oscillatory mechatronic systems," *IEEE International Conference on Emerging Technologies and Factory Automation, ETFA*, vol. 2019-Septe, pp. 829–835, 2019.

[6] Y. Chen, M. Yang, J. Long, K. Hu, D. Xu, and F. Blaabjerg, "Analysis of Oscillation Frequency Deviation in Elastic Coupling Digital Drive System and Robust Notch Filter Strategy," *IEEE Transactions on Industrial Electronics*, vol. 66, no. 1, pp. 90–101, 2019.

[7] Y. Fu, M. Yang, Q. Ni, and D. Xu, "Mechanical resonance suppression and disturbance rejection of 2-inertia system with observer-based feedback control," *2016 IEEE 8th International Power Electronics and Motion Control Conference, IPEMC-ECCE Asia 2016*, pp. 3084–3088, 2016.

[8] M. Yang, W. Zheng, K. Yang, and D. Xu, "Suppression of mechanical resonance using torque disturbance observer for two-inertia system with backlash," *9th International Conference on Power Electronics - ECCE Asia: "Green World with Power Electronics", ICPE 2015-ECCE Asia*, pp. 1860–1866, 2015.

[9] M. Yang, C. Wang, D. Xu, W. Zheng, and X. Lang, "Shaft Torque Limiting Control Using Shaft Torque Compensator for Two-Inertia Elastic System With Backlash," *IEEE/ASME Transactions on Mechatronics*, vol. 21, no. 6, pp. 2902–2911, 2016.

[10] Y. Qiao, J. Cao, and C. Ma, "Transient response control of two-mass system via polynomial approach," *Journal of Dynamic Systems, Measurement and Control, Transactions of the ASME*, vol. 136, no. 6, 2014.

[11] M. Goubej and M. Schlegel, "PI Plus Repetitive Control Design: H-infinity Regions Approach," pp. 62–67, 2019.

[12] M. Čech, A. J. Beltman, and K. Ozols, "I-MECH - Smart System Integration for Mechatronic Applications," *IEEE International Conference on Emerging Technologies and Factory Automation, ETFA*, vol. 2019-Septe, pp. 843–850, 2019.

[13] A. I. Petros and S. Jing, *Robust adaptive control*. Mineola: Dover Publications, Inc., 2012.

[14] P. Blaha and P. Vaclavek, "Adaptive deadbeat current controllers for AC induction motor control," *PECon 2008 - 2008 IEEE 2nd International Power and Energy Conference*, no. PECon 08, pp. 712–717, 2008.

[15] O. Bartik and L. Buchta, "Angle tracking observer for the velocity estimation with the filtered control variable," *IFAC-PapersOnLine*, vol. 52, no. 27, pp. 496–501, 2019.